Vol. 62: 293–306, 1990 | MARINE ECOLOGY PROGRESS SERIES
Mar. Ecol. Prog. Ser. | Published April 19

Some effects of iron and nitrogen stress on the red tide dinoflagellate *Gymnodinium sanguineum*

Gregory J. Doucette*, Paul J. Harrison

Departments of Oceanography and Botany, University of British Columbia, Vancouver, British Columbia, Canada V6T 1W5

ABSTRACT: Growth rate (μ), cell volume (CV), chlorophyll *a* quota (Q_{chl}), and in vivo fluorescence (F) and DCMU-enhanced F (F_D) were measured in Fe-limited, semi-continuous cultures of *Gymnodinium sanguineum*, which varied free ferric ion activity (pFe; i.e. – log free ferric ion activity) from 16.0 to 22.2, and in Fe-deplete batch cultures. Selected variables were also determined for cultures grown into nitrogen depletion. The majority of Fe-limited cellular characteristics changed most rapidly over the same pFe range (20.2 to 21.2), with μ, CV and Q_{chl} declining, while F/chl *a* and F_D/chl *a* increased. The half-saturation constant for iron-limited growth (K_μ) was near the maximum of values calculated for other neritic species examined previously. More importantly, however, the competitive ability of *G. sanguineum* (as indicated by μ_{max}/K_μ, the slope of the Monod equation at lowest substrate concentrations) under conditions of severe iron stress was lowest of the 10 species considered. Fe and N depletion affected Q_{chl} similarly, while the former caused a markedly greater increase in F/chl *a* and F_D/chl *a*. Enhancement of in vivo fluorescence demonstrates the adverse effects of Fe stress on the utilization of harvested light energy. Because of the extent to which Fe limitation modified F/chl *a* and the distinction from N-mediated changes, this ratio, in conjunction with other probes of nutritional status, may be a useful indicator of Fe-stressed red tide populations. Ultrastructural observations of Fe-deplete cells showed reductions in chloroplast number and some degeneration of lamellar organization, both of which provide a structural basis for changes noted in Q_{chl} and fluorescence properties.

INTRODUCTION

Marine phytoplankton require a variety of trace metals (e.g. Fe, Mn, Zn, Ni, Cu) for cell maintenance and growth. Depending on the element, concentrations in coastal regions can exceed those of oceanic waters by as much as 4 orders of magnitude (Brand et al. 1983). Recent work has established a distinction in trace metal-limited growth rates between neritic and oceanic phytoplankton species (Brand et al. 1983, Murphy et al. 1984). The clearest pattern for those metals compared (i.e. Fe, Mn, Zn) was observed under iron limitation. All neritic species exhibited significant reductions in growth rate below the same substrate concentration, whereas the reproduction of oceanic species was generally not (or only slightly) limited at any Fe level tested. Unfortunately, no dinoflagellates were among those coastal species considered.

It has been suggested that dinoflagellates may account for 30% of total productivity in the world's oceans (Yentsch et al. 1980). Included in this ecologically diverse group are species capable of producing red tides, virtually monospecific blooms in which cell densities often surpass 10^6 cells l^{-1} (Taylor 1987). Red tide dinoflagellates can be either toxic or non-toxic. Because blooms of either type can result in the death of marine organisms (Steidinger & Haddad 1981, Taylor 1987), these phenomena are of particular ecological significance. Although research continues into the nutritional factors which regulate the population dynamics of these organisms, some evidence suggests that iron bioavailability may be important in this regard (e.g. Ingle & Martin 1971, Glover 1978, Yamochi 1984). There is clearly a need for more information on the iron nutrition of dinoflagellates in general and, specifically, of red tide species. Thus, a principal objective of this work was to investigate the growth of a red tide dinoflagellate, *Gymnodinium sanguineum* Hirasaka, under iron-limiting conditions. This non-toxic species is considered taxonomically synonymous with *G. splendens*

* Present address: Biology Department, Woods Hole Oceanographic Institution, Woods Hole, Massachusetts 02543, USA

0171-8630/90/0062/0293/$ 03.00

Lebour and *G. nelsoni* Martin (Tangen 1979), and frequently predominates in red tides occurring throughout the world's coastal waters (e.g. Dandonneau 1970, Rojas de Mendiola 1979, Robinson & Brown 1983).

Other effects of iron limitation on which few data exist for dinoflagellates are alterations to cellular compounds in which iron is either a constituent or required for biosynthesis. The role of iron in photosynthesis is essential. It is a component of photosynthetic electron transfer (PET) reactions in the form of cytochromes and iron-sulfur proteins (e.g. ferredoxin), and is necessary for the biosynthesis of chlorophyll pigments (see Reuter & Peterson 1987). Previous investigations of iron-mediated changes in algal pigments and characteristics associated with PET have employed diatoms and chrysophytes (Glover 1977, Sakshaug & Holm-Hansen 1977), cyanobacteria (Guikema & Sherman 1983, Sandmann & Malkin 1983), and a chlorophyte (Verstreate et al. 1980). The present study examines the effects of iron limitation and depletion on chlorophyll *a* quota (Q_{chl}) and PET processes (as determined by in vivo fluorescence properties) in semi-continuous and batch cultures of a dinoflagellate. Since nitrogen is a constituent of both chlorophyll pigments and PET components, variations similar to those occurring under iron stress might also be expected. Thus, to provide additional support for the specificity of iron stress-mediated changes in these variables (i.e. Q_{chl} and in vivo fluorescence), the same measurements were made on batch cultures grown into nitrogen depletion.

Alterations in the photosynthetic apparatus and general cell ultrastructure as a result of iron deficiency have been reported for several algal species (e.g. Meisch et al. 1980, Douglas et al. 1986, Hilt et al. 1987) including one dinoflagellate (Doucette & Harrison 1989). Such information allows a more direct structural interpretation of an organism's biochemical or physiological response to a given stimulus. As a final part of this study the ultrastructure of iron-replete and iron-deplete *Gymnodinium sanguineum* cells was examined. Observations are compared with results from the literature, including those presented by Doucette & Harrison (1989) for another red tide dinoflagellate *(Alexandrium tamarense)*, and are also considered with regard to chl *a* and in vivo fluorescence data.

MATERIALS AND METHODS

General culture maintenance. Stock cultures of *Gymnodinium sanguineum* (Culture # D354, North East Pacific Culture Collection, Dept of Oceanography, University of British Columbia) were maintained on filter-sterilized (Millipore 0.45 μm), ESAW-enriched artificial seawater (Harrison et al. 1980) with several adjustments to the original medium. Silicon was omitted while $Na_2glyceroPO_4$ and $FeNH_4(SO_4)_2$ $6H_2O$ were replaced by equimolar concentrations of Na_2HPO_4 and $FeCl_3$ $6H_2O$, respectively. Na_2MoO_4 $2H_2O$ was added at a concentration of 0.52 μM. Deionized distilled water (DDW) and reagent grade chemicals were used in preparing salt and nutrient enrichment solutions. Culture vessels employed throughout this research were soaked in freshly made 10 % HCl (v/v) for at least 2 to 3 d and rinsed thoroughly with DDW prior to use. All cultures (i.e. stock and experimental) were grown at 17 °C without stirring, due to this species' sensitivity to physical perturbation (Doucette 1988). Continuous illumination was supplied by Vita-Lite® UHO fluorescent tubes filtered through blue Plexiglas® (No. 2069, Rohm and Haas) at an irradiance of 145 μE m^{-2} s^{-1} (saturating for growth of *G. sanguineum;* Doucette 1988).

Iron and nitrogen depletion. Media used to achieve iron (−Fe ESAW) or nitrogen (−N ESAW) depletion were modifications of stock maintenance ESAW, with residual trace metal contamination minimized by treatment with Chelex 100 ion exchange resin (Morel et al. 1979). Iron was omitted from −Fe ESAW. EDTA was combined with the remaining trace metals and its concentration reduced to provide an EDTA:trace metal ratio of 1.6. Final micromolar concentrations of metals added were as follows: Mn, 2.42; Zn, 0.25; Co, 5.69 × 10^{-2}; Mo, 0.52. −N ESAW contained no added nitrogen. Media were acidified to ca pH 5.5 using Suprapur® HCl (Merck), sterilized by autoclaving, and reequilibrated to ca pH 8.1 by bubbling with sterile (Millipore 0.22 μm) air. Chelexed filter-sterilized (Millipore 0.22 μm) $NaHCO_3$ was then added at a final concentration of 2 mM to avoid possible carbon limitation at high batch culture cell densities.

Iron (triplicate cultures) and nitrogen (single culture) depletion experiments were carried out in 2.8 l polycarbonate (PC) Fernbach flasks and initiated by inoculating with early stationary phase stock cultures to ca 100 cells ml^{-1}. Continuous bubbling with sterile (Millipore 0.22 μm) air or 1 to 2 % CO_2 was required to avoid growth inhibition by pH prior to depletion of biologically available iron in −Fe cultures (pH range 8.1 to 8.8, avg. ca 8.4, terminal value ca 8.2). Several variables, including cell density (CD), average cell volume (CV), chlorophyll *a* (chl *a*), and in vivo fluorescence (F) and DCMU-enhanced F (F_D), were monitored during the course of an experiment (see below for details). Values for nutrient-deplete (−Fe or −N) cultures correspond to cellular exhaustion of the growth-limiting nutrient as determined by no change or a decrease in CD on successive days. It is presumed that cell quotas of the limiting nutrient approach a minimum value at this time. Depletion of the desired nutrient was confirmed

for both −Fe and −N cultures by bioassay and, in the case of the latter, by monitoring ambient NO_3 concentrations.

Iron-limited growth. Preparation of media was the same as described for iron depletion experiments except that following sterilization, ESAW $NaHCO_3$ concentrations were not supplemented. Also, the following changes in EDTA and trace metal enrichments were made. Six types of ESAW media, with EDTA and trace metals based on the formulation of Brand et al. (1983), were designed to achieve a range of iron-limited (as well as an iron-replete) growth conditions by varying free ferric ion activities. EDTA and iron ($FeCl_3$ $6H_2O$) were combined in single solutions, with iron adjusted to provide final total molar concentrations (Fe_{total}) of 10^{-9}, 10^{-8}, 10^{-7}, 10^{-6}, 10^{-5} and 10^{-4} (= iron-replete). The remaining trace metals were prepared as one stock solution without EDTA. Iron and other trace metal free ion activities were buffered by maintaining the final EDTA concentration at 10^{-4} M.

Transition metal free ion activities for each of the 6 media types (Table 1) were calculated using the chemical equilibrium program MINEQL (Westall et al. 1976) and the stability constants of Ringbom (1963) for an ionic strength of 0.7 at pH 8.1. Computations take into account all changes in original ESAW enrichments and thus provide reasonable estimates of pFe (i.e. negative log free ferric ion activity) for this system, based on the conditions and stability constants invoked. Actual pFe values will, however, tend to exceed those estimated by the MINEQL program due to the photoreduction of Fe(III)-EDTA [liberated Fe(II) is oxidized rapidly to Fe(III) which is recomplexed slowly by EDTA] in the illuminated cultures. It should also be recognized that the maximum error in pFe calculations will be associated with the lowest and highest iron additions due to the questionable assumption of no iron contamination and to the addition of equimolar iron and EDTA, respectively. The latter, more poorly buffered system, exhibits a greater tendency for iron precipitation and higher free ion activities of other transition metals (see Table 1).

Experiments were run in duplicate as unbubbled, semi-continuous cultures (85 ml polycarbonate Oak Ridge tubes, Nalgene) established by transferring iron-deplete cells into each of the 6 iron concentrations. Cultures were maintained in exponential phase (ca 100 to 600 cells ml^{-1}; pH range 8.0 to 8.3) by dilution with fresh medium, and specific growth rates calculated based on changes in cell density. Growth rates for each pFe represent an average of 6 to 12 sequential growth curves among which doubling times varied by less than ca 15%. Kinetic parameters of maximum growth rate (μ_{max}) and half-saturation constant for growth (K_μ) were estimated using a non-linear curve-fitting program (Labtec Notebook Curvefit®, Laboratory Technologies Corp.) which fits data directly to a specified model through an iterative, least-squares regression technique. The model chosen in this case was the Monod equation:

$$\mu = \mu_{max} (S/K_\mu + S) \quad (1)$$

where μ = specific growth rate; μ_{max} = maximal growth rate; S = molar substrate concentration; and K_μ = S at half-maximal growth rate. Values of μ_{max} and K_μ were also derived from a Hanes-Woolf linear transformation of the data according to the equation:

$$S/\mu = K_\mu/\mu_{max} + (1/\mu_{max}) S \quad (2)$$

Variable definitions are the same as those given for Eq. (1). Approximate steady-state determinations of chl *a*, F, and F_D were made twice on duplicate cultures of each pFe following an acclimation period of at least 6 or 7 generations.

Analytical methods. Cell counts were performed on a Coulter Counter® model TAII (200 μm aperture, 44.2 μm calibration spheres), with data for average cell volume obtained simultaneously from a particle size distribution based on equivalent spherical diameter. Chl *a* concentration of filtered samples (gravity filtration, Whatman 934-AH) was determined fluorometrically (Holm-Hansen et al. 1965) in 90% acetone extracts (20 h, 4 °C) using a Turner Designs® model 10 fluorometer (Corning filters: 3–66, reference; 5–60, excitation; 2–64, emis-

Table 1. Molar free ion activities of metals added to iron-limited growth media. Calculations were performed with MINEQL (Westall et al. 1976) and are based on the stability constants of Ringbom (1963). 10^{-4} M EDTA was present in all media

pFe_{total}[a]	pFe[b]	pMn	pZn	pCu	pCo
4.0	16.0	7.6	9.6	12.9	10.4
5.0–9.0[c]	18.2–22.2[d]	8.4	10.9	14.2	11.7

[a] Negative log of total iron concentration
[b] Negative log of free ferric ion activity
[c] Range includes individual values of 5.0, 6.0, 7.0, 8.0, 9.0
[d] Range includes individual values of 18.2, 19.2, 20.2, 21.2, 22.2

sion). In vivo F and F_D measurements of dark-equilibrated (20 min, see Loftus & Seliger 1975) culture aliquots employed the fluorometer and filters used for chl *a* determinations. Samples for F_D were treated with aqueous 10^{-5} M (final concentration) 3-(3,4 dichlorophenyl)-1,1-dimethylurea (DCMU) prior to dark equilibration. Readings were taken following 30 s exposure to the fluorometer light source. Ambient NO_3 concentrations (NO_3 + NO_2) in the −N batch culture were measured with a Technicon Autoanalyzer® II according to the procedure of Wood et al. (1967).

Ultrastructure. Iron-replete and iron-deplete cultures were sampled for transmission electron microscopy (TEM) by collecting cells on 2 μm Millipore filters (type BS) and processing as follows: primary fixation with 1.5% glutaraldehyde in 0.1 M sodium cacodylate and 0.4 M sucrose (2 h, room temp.), and post-fixation with 1% osmium tetroxide in 0.1 M sodium cacodylate (1 h, room temp.). Samples were stained en bloc using 1% aqueous uranyl acetate, dehydrated in a graded ethanol/propylene oxide series, and embedded in Epon 812. A diamond knife was used to cut random and serial sections which were picked up on formvar-coated 50-mesh copper grids, stained with saturated uranyl acetate (in 50% methanol) and lead citrate, and examined in a Zeiss EM10C transmission electron microscope.

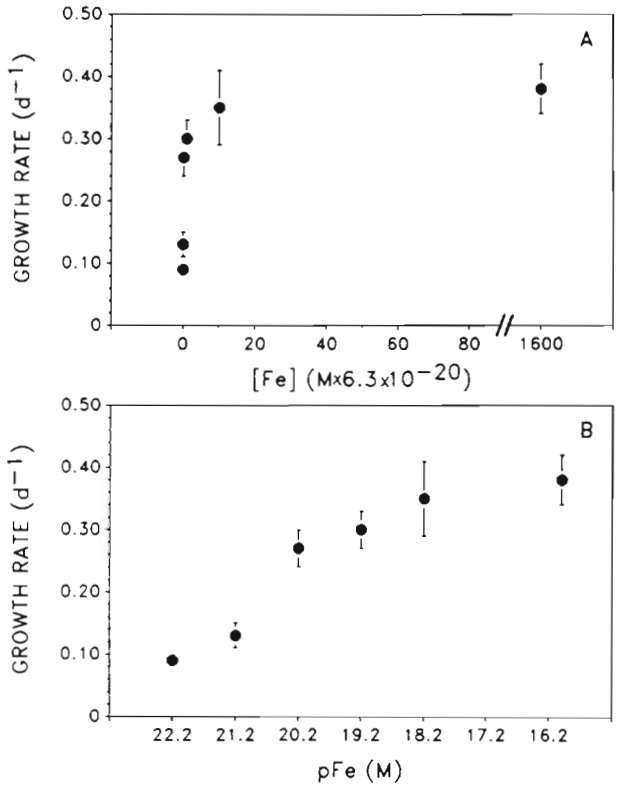

Fig. 1 *Gymnodinium sanguineum*. (A) Linear and (B) semi-log plots of growth rate as a function of free ferric ion activity. Molar free ferric ion activities in (A) may be determined by multiplying the plotted value by 6.3×10^{-20}. Also, note scale break between the 2 highest activities in (A). Error bars = ± 1 SD (n = 6 to 12), and are smaller than symbol where not apparent

RESULTS

Iron-limited growth

Specific growth rates of *Gymnodinium sanguineum* as a function of free ferric ion activity are presented in linear (Fig. 1A) and semi-log (Fig. 1B) plots. The more conventional linear graph demonstrates the hyperbolic relationship between growth rate (μ) and substrate concentration (S). The kinetic parameters for iron-limited growth, as estimated by a direct fit of these data to the Monod equation using the Curvefit® program, were a maximum growth rate (μ_{max}) of 0.34 d^{-1} and a half-saturation constant (K_μ) of 1.0×10^{-21} (Table 2). By comparison, a Hanes-Woolf linear transformation, which plots S/μ against S (not shown), yielded values of 0.38 d^{-1} and 1.7×10^{-20} for μ_{max} and K_μ, respectively (Table 2). Although perhaps not obvious in Fig. 1A, a semi-log plot of μ vs S (Fig. 1B) shows clearly that the most critical S interval occurs between pFe 20.2 ($Fe_{total} = 10^{-7}$) and 21.2 ($Fe_{total} = 10^{-8}$). As free ferric ion activity decreased over this range μ declined from 0.27 to 0.13 d^{-1}, a difference at least twice that observed between any other adjacent substrate concentrations.

With the exception of the fluorescence index $1 - F/F_D$, all variables and their ratios remained essentially constant between pFe 16.0 and 20.2, but changed markedly as free ferric ion activity decreased from $10^{-20.2}$ to $10^{-21.2}$. While average cell volume (Fig. 2) declined by 35% over this interval, Q_{chl} (Fig. 3) was reduced by half. Conversely, both F and F_D normalized per unit chl *a* (Fig. 4A) were ca 2-fold greater at pFe 21.2 than at 20.2. $1 - F/F_D$ (Fig. 4B) showed a generally decreasing trend with increasing iron stress.

Iron and nitrogen depletion

Iron depletion (i.e. terminal point of a batch culture) caused all cellular characteristics monitored (Figs. 2 to 4) to change in the same relative direction as with increasingly Fe-limited growth (i.e. semi-continuous cultures) below pFe 20.2. Iron-deplete and the most Fe-limited cells (pFe 22.2) differed to the largest extent (ca 2-fold) in Q_{chl} (0.16 and 0.29 g l cell vol.$^{-1}$, respectively; Fig. 3) and F/chl *a* (320 and 150, respectively; Fig. 4A).

Comparison of iron- and nitrogen-deplete cells showed similar measurements of CV (Fig. 2) and Q_{chl}

Table 2. Estimates of μ_{max} (d^{-1}) and K_μ (M) for iron-limited growth of 10 neritic phytoplankton species using the non-linear curve-fitting program Curvefit[R] (the Monod equation was chosen as the theoretical model to which the data were fit directly). Values in parentheses were derived from a Hanes-Woolf linear transformation of the same data. Also given are μ_{max}/K_μ ratios, which represent the initial slope of the Monod equation for a given species (see text for details)

Species	μ_{max}	K_μ	μ_{max}/K_μ	Source
Dinophyceae				
Gymnodinium sanguineum	0.34 (0.38)	1.0×10^{-21} (1.7×10^{-20})	3.4×10^{20}	(1)
Bacillariophyceae				
Asterionella glacialis	1.19	4.4×10^{-22}	2.7×10^{21}	(2)
Bacteriastrum hyalinum	0.80	4.1×10^{-23}	2.0×10^{22}	(2)
Ditylum brightwellii	0.96	2.1×10^{-22}	4.6×10^{21}	(2)
Lithodesmium undulatum	1.04	1.2×10^{-21}	8.7×10^{20}	(2)
Skeletonema costatum	1.32	3.1×10^{-22}	4.3×10^{21}	(2)
Streptotheca tamesis	0.93	1.3×10^{-22}	7.2×10^{21}	(2)
Thalassiosira pseudonana	1.21	3.9×10^{-22}	3.1×10^{21}	(2)
Thalassiosira weissflogii	1.99	3.2×10^{-21}	6.2×10^{20}	(3)
Haptophyceae				
Hymenomonas carterae	0.68	1.9×10^{-22}	3.6×10^{21}	(2)

Sources: (1) This study; (2) Brand et al. (1983): pFe values given were recalculated using MINEQL (Westall et al. 1976) and the stability constants of Ringbom (1963) prior to linear transformation (see text for explanation); (3) data from Harrison & Morel (1986, Fig. 1)

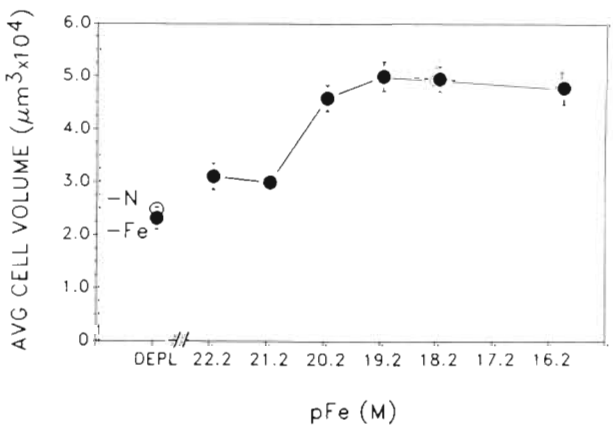

Fig. 2. *Gymnodinium sanguineum*. Average cell volume as a function of free ferric ion activity, and iron or nitrogen depletion. In Figs. 2 to 4: iron (−Fe) and nitrogen (−N) deplete cultures are plotted before the scale break; n = 2 for Fe-limited data, n = 3 for Fe-deplete point, n = 1 for N-deplete point; error bars = ± 1 SD and are smaller than symbol where not apparent for n ≥ 2

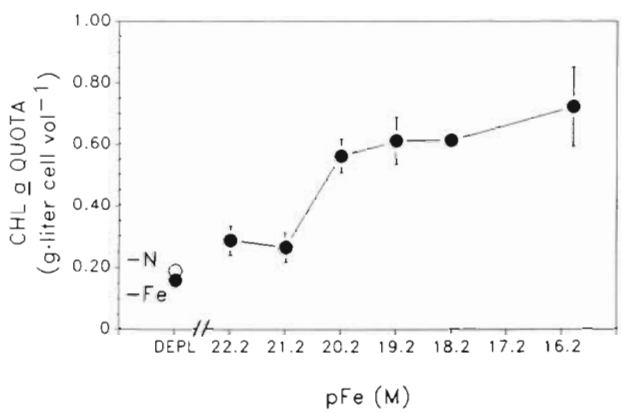

Fig. 3. *Gymnodinium sanguineum*. Chlorophyll *a* quota as a function of free ferric ion activity, and iron or nitrogen depletion. Symbol labels, sample size and error bars as in Fig. 2

(Fig. 3). The most notable distinction between Fe and N depletion occurred in ratios of which F and, to a lesser degree, F_D were components. F/chl *a* (Fig. 4A) and F_D/chl *a* (Fig. 4A) of Fe-deplete cells exceeded N-deplete values by 2.5-fold (ca 160 %) and 1.6-fold (ca 60 %), respectively. Further, the F/chl *a* ratio of N-deplete cells (125, Fig. 4A) was ca 20 % less than for the most Fe-limited condition (pFe 22.2). Nitrogen depletion resulted in a less than 10 % decrease of $1 - F/F_D$ below the nutrient-replete index (i.e. from 0.68 to 0.62), as compared to 43 % (0.39) for Fe depletion (Fig. 4B).

In the absence of available chl *a* and in vivo fluorescence data for a range of N-limited semi-continuous cultures, Figs. 5 and 6 show changes in ratios of these variables during batch culture growth into nitrogen depletion. Comparable data for iron depletion were also obtained (Figs. 5 and 6). Ambient NO_3 was undetectable in the −N culture by Day 9 (Fig. 5). Thus, moderately N-deficient conditions (i.e. continuing cell division in the absence of ambient NO_3) were associated with Day 12, while Day 14 represented either

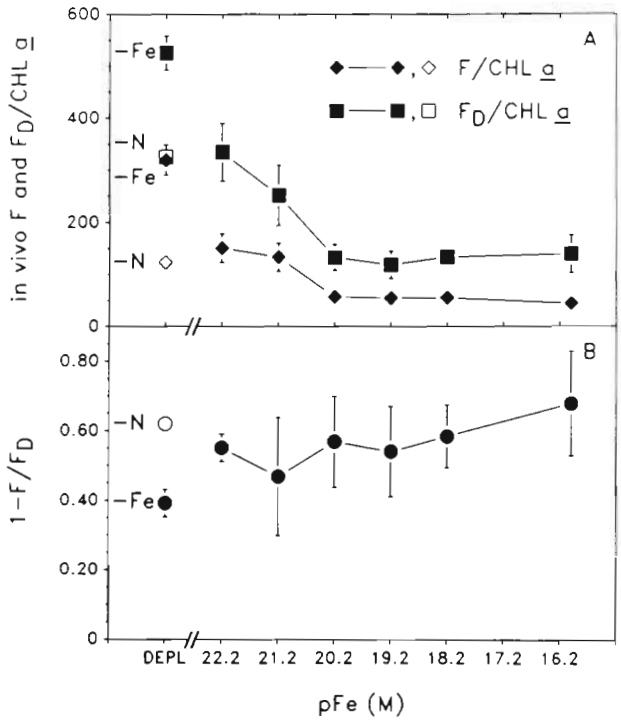

Fig. 4. *Gymnodinium sanguineum*. (A) In vivo fluorescence (F) and DCMU-enhanced fluorescence (F_D) expressed per unit chl *a*; (B) 1 − F/F_D as a function of free ferric ion activity, and iron or nitrogen depletion. Symbol labels, sample size and error bars as in Fig. 2

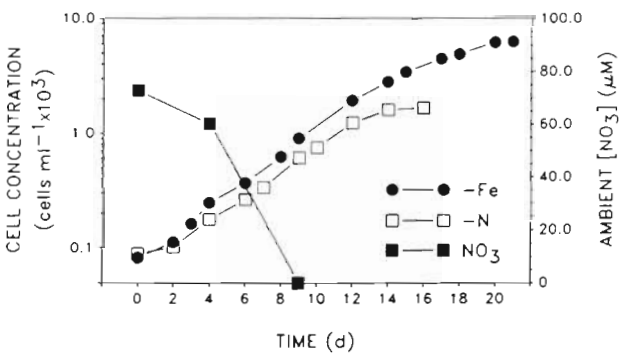

Fig. 5. *Gymnodinium sanguineum*. Changes in cell concentration over time for batch cultures grown into iron (−Fe) or nitrogen (−N) depletion. Concurrent changes in ambient NO_3 concentration are shown for the −N culture

severe N deficiency or depletion (i.e. cessation of cell division). Under conditions of moderate N deficiency (Day 12), F/chl *a* (Fig 6A) and F_D/chl *a* (Fig. 6B) were only ca 25 % greater (F/chl *a*, 65; F_D/chl *a*, 165) than for logarithmically growing cells (Day 4). By Day 14 more notable increases in both ratios to within ca 15 % of terminal values (Day 16: F/chl *a*, 125; F_C/chl *a*, 325) had occurred. 1 − F/F_D (Fig. 6C) remained between 0.58 and 0.69, irrespective of culture nitrogen status. In

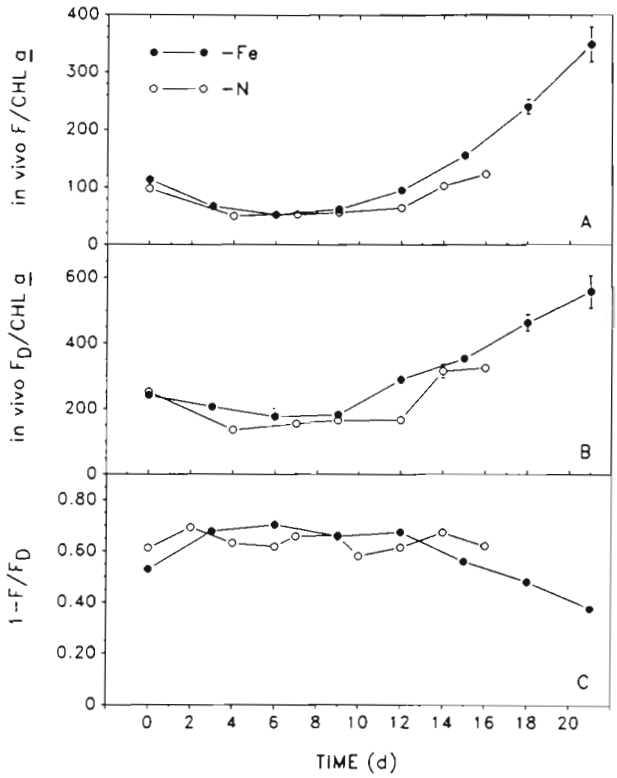

Fig. 6. *Gymnodinium sanguineum*. Plots of (A) in vivo fluorescence (F)/chl *a* , (B) DCMU-enhanced F (F_D)/chl *a*, and (C) 1 − F/F_D over time for batch cultures (shown in Fig. 5) grown into iron (−Fe) or nitrogen (−N) depletion. Values plotted for each culture are mean ± 1 SD for duplicate determinations of each variable; error bars are smaller than symbol where not apparent

contrast to N stress, F/chl *a* (Fig. 6A) and F_D/chl *a* (Fig. 6B) of the −Fe culture began to rise during mid-exponential phase (Day 9), with both ratios exceeding terminal N depletion measurements by Day 15 (F/chl *a*, 155; F_D/chl *a*, 355). 1 − F/F_D (Fig. 6C) lagged the response of F/chl *a* and F_D/chl *a* by ca 3 d and, conversely, declined to below N-deplete (terminal) values by Day 15 (0.56). Ambient iron concentrations, and thus estimates of iron status, were not determined during −Fe culture growth.

Ultrastructure

Iron-replete protoplasts (Fig. 7) were characterized by extensive vacuolar space interspersed with regions of cytoplasm, and a prominent nucleus containing numerous permanently-condensed chromosomes. Another distinctive structure was the pusule system (Fig. 8), a reticulate vacuolar network surrounding the area of flagellar insertion (Fig. 9). Whether the pusule system comprised 1 or 2 pusules (see Taylor 1990),

could not be distinguished. Vesicle activity was concentrated more toward the cell surface (Figs. 8 and 10) and around the longitudinal flagellar canal (Fig. 9). Numerous chloroplasts and mitochondria, as well as dense aggregates of endoplasmic reticulum (most notably rough ER), occurred closely grouped throughout the cell, while starch and lipid reserves were restricted primarily to cortical regions (Figs. 7 and 11). One or 2 accumulation bodies, often comprising tightly-packed material in a 'fingerprint'-like pattern, were present in some cells (Figs. 7 and 12). Chloroplasts exhibited lamellae consisting of 2 or 3 appressed thylakoids (Fig. 13). Mitochondria contained tubular cristae within a granular matrix, similar in electron density to the surrounding cytoplasm (Fig. 11).

Iron-deplete protoplasts (Fig. 14) were considerably different from those growing under iron-replete conditions (Fig. 7), as demonstrated by comparing similar whole-cell longitudinal sections. Most obvious was a decline in the cytoplasm to vacuole ratio. Vacuolar regions occupied much of the cell periphery and were compartmentalized by the tonoplast (Fig. 14). Organelles remained in close association within the available cytoplasm; however, the abundance of ER was apparently reduced (Fig. 15). Also characteristic of Fe-deplete cells was a notable (albeit unquantified) decrease in chloroplast number (Fig. 14). Thylakoids occurred in pairs or singly (cf. Figs. 11 and 13). Degenerative structural changes were evident in the separation of adjacent thylakoids (Fig. 15) and the dilation of individual thylakoids (Fig. 16). Many chloroplast lamellae (and their constituent thylakoids) did, however, retain a 'normal' appearance (Fig. 15), and no clear difference in the number of lamellae per chloroplast was discernible. Alterations in mitochondrial morphology associated with iron depletion appeared predominantly as reductions in electron density of the matrix (Fig. 15, cf. Fig. 11). Accumulation body contents of Fe-deplete cells (Fig. 17) were loosely arranged and showed no pattern or structural organization (cf. Fig. 12).

DISCUSSION

Iron-limited growth kinetics

Our work is the first to examine iron-limited growth in a coastal red tide dinoflagellate *(Gymnodinium sanguineum)*. Growth rates of several coastal diatom species and a neritic coccolithophorid, as a function of iron bioavailability, have been examined previously (Brand et al. 1983, Harrison & Morel 1986). Although meaningful comparisons are possible among these data, it is first necessary to account for differences between pFe values given in Brand et al. (1983), and those provided herein and also by Harrison & Morel (1986). Metal free ion activities are determined largely by how a system is defined (e.g. ionic strength, pH, etc.) and the stability constants of chemical species present, and can vary considerably depending on the data input to satisfy these criteria (Kester 1986). Media formulations used in the present study and by Brand et al. (1983) are very similar; however, estimates of free ferric ion activities based on the stability constants of Ringdom (1963) and Sillen & Martell (1964), respectively, differ by an order of magnitude (higher in the former case). For purposes of this discussion, pFe calculations of Brand et al. (1983) will be considered as 10-fold underestimates to allow direct comparison of kinetic constants for iron-limited growth. In other words, while erroneous values are not inferred for either study, pFe 20.2 of Brand et al. (1983), for example, is taken as equivalent to pFe 19.2 herein. Values of pFe given by Harrison & Morel (1986) are roughly equivalent to those determined herein, as free ion activities of both media were calculated using MINEQL (Westall et al. 1976) with similarly defined systems and the stability constants of Ringbom (1963).

Iron-limited growth of *Gymnodinium sanguineum* is similar to that reported for other neritic phytoplankton (Brand et al. 1983, Harrison & Morel 1986) in that all growth rates begin to decline rapidly below pFe 20.2. However, a more critical comparison of these data is possible based on the kinetic parameters μ_{max} and K_μ. Each of these growth constants was estimated for *G. sanguineum* using both a non-linear curve-fitting program, Curvefit®, and a Hanes-Woolf linear transformation. We also employed Curvefit® to determine μ_{max} and K_μ for the 9 coastal species examined by Brand et al. (1983) using the numerical data provided in their paper. It was assumed that the maximum growth rate had been achieved for these species since μ varied by 10 % or less between the 2 highest substrate concentrations in all but one case, which was therefore not considered. Although values of μ_{max} and K_μ for *Thalassiosira weissflogii* derived from a Hanes-Woolf plot were presented by Harrison & Morel (1986, their Table 2), we applied the Curvefit® program to their data (their Fig. 1) in order to obtain estimates of these kinetic parameters which would be more directly comparable to those calculated herein.

Estimated values of μ_{max} and K_μ for the iron-limited growth of 10 neritic phytoplankton species are given in Table 2. Maximum specific growth rates range ca 6-fold from 0.34 (*Gymnodinium sanguineum*) to 1.99 (*Thalassiosira weissflogii*) d^{-1}, while the molar free ferric ion activity which limits growth of a species by half ranges ca 2 orders of magnitude from 4.1×10^{-23} M (*Bacteriastrum hyalinum*) to 3.2×10^{-21} M (*T. weissflogii*). Discussions of kinetic constants usually consider

estimates generated by a linear transformation of the Monod equation. However, a Hanes-Woolf plot of our data yielded a K_μ (1.7×10^{-20} M) 10 times that calculated with the non-linear curve-fitting program Curvefit®, and clearly overestimated the substrate concentration corresponding to one-half μ_{max} (see Fig. 1). In view of this and other potential problems associated with obtaining kinetic constants of Monod-type equations from linear transformations (Li 1983, Robinson & Characklis 1984), we will consider further only those

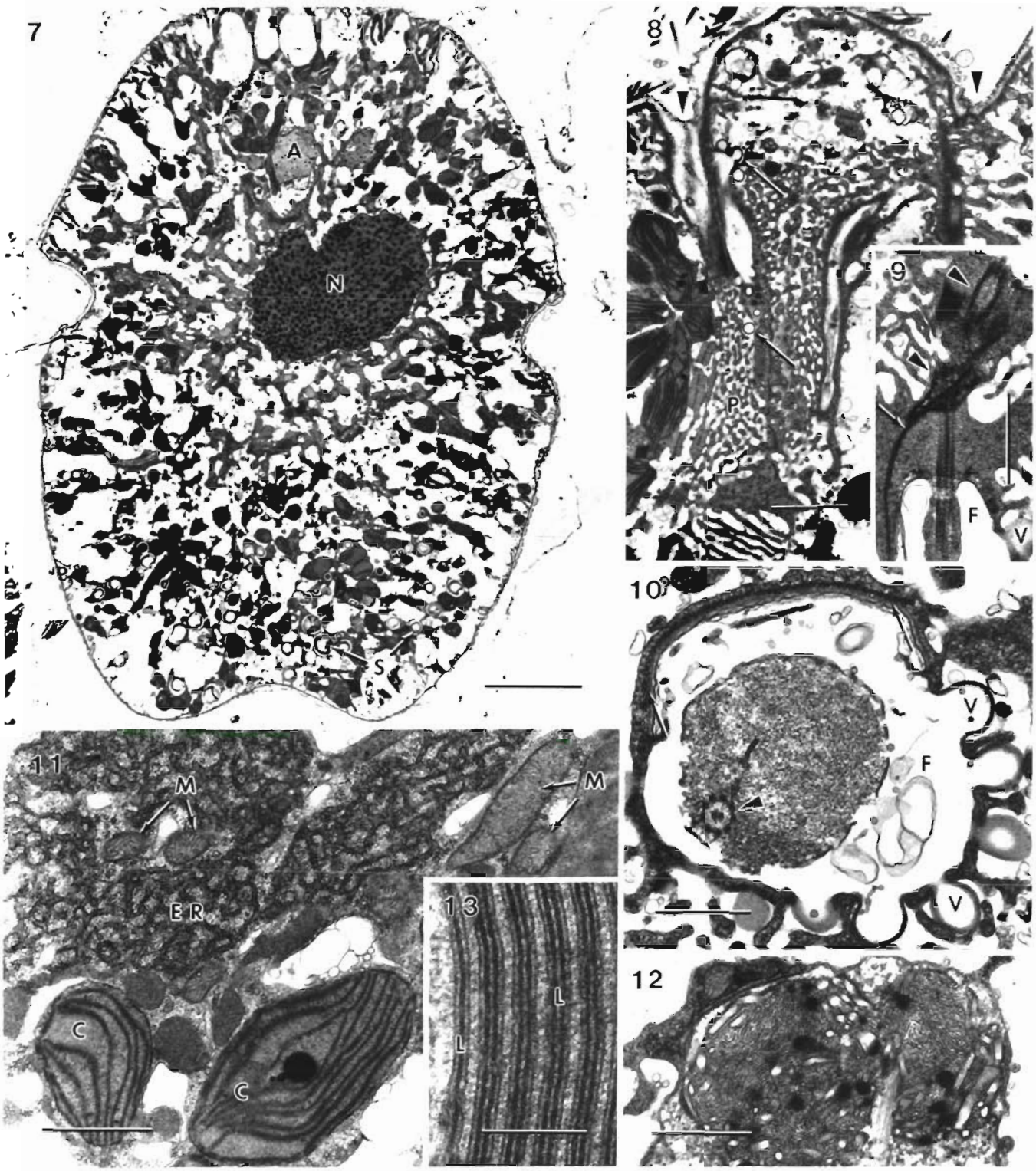

values derived from fitting data directly to the Monod equation using Curvefit®.

Estimates of K_μ for the dinoflagellate *Gymnodinium sanguineum* (1.0×10^{-21} M) and 2 diatoms, *Lithodesmium undulatum* (1.2×10^{-21} M) and *Thalassiosira weissflogii* (3.2×10^{-21} M), exceeded all others by more than 2-fold (Table 2), indicating that iron-limited growth would occur at greater free ferric ion activities in these 3 species. One might also conclude on the basis of half-saturation constants alone that *T. weissflogii,* with the largest K_μ, would be competitively inferior to all other species (Table 2) under conditions of severe iron stress. It is, however, the growth rate at low substrate concentrations which should exert the dominant influence on the outcome of competition as nutrient supply becomes limiting.

The ratio μ_{max}/K_μ (i.e. slope of the Monod equation at lowest substrate concentrations) has been suggested by Healey (1980) to be a reasonable indicator of differences in growth rate at low S values (lower ratios indicating lower growth rates), and we have therefore calculated this index for those species listed in Table 2. Since lower μ_{max}/K_μ ratios are (to a first approximation) indicative of inferior competitive ability, the dinoflagellate *Gymnodinium sanguineum* ($\mu_{max}/K_\mu = 3.4 \times 10^{20}$; lowest value by ca 2-fold) would appear to be the species least likely to outcompete the other predominantly diatom species under conditions of reduced iron bioavailability. This contention is supported not only by Healey's (1980) finding that approximately a doubling of μ_{max}/K_μ represents a doubling of growth rate at lowest substrate concentrations, but also by the roughly 3-fold higher growth rate of *Thalassiosira weissflogii* ($\mu_{max}/K_\mu = 6.2 \times 10^{20}$; value closest to *G. sanguineum*) over *G. sanguineum* at the lowest common iron concentration examined (*T. weissflogii* data from Fig. 1 of Harrison & Morel 1986). While these data do not confirm a role of iron in regulating the natural population dynamics of *G. sanguineum,* they do suggest that this red tide species may be more susceptible (in terms of growth limitation and competitive ability) to iron stress than many other coastal phytoplankters.

Cell volume, chl *a* quota, and in vivo fluorescence

CV, Q_{chl}, and F and F_D/chl *a* determinations are consistent with those of growth rate in identifying pFe 20.2 to 21.2 as the most critical range of substrate concentrations. Changes in these variables were clearly associated with iron-limited growth. However, comparable responses have been observed with other forms of environmental stress and, in certain cases, a more generalized response to lower growth rates must be considered as a possible explanation. For example, while iron depletion reduced CV by ca 60 %, nitrogen depletion or low irradiance levels (Doucette 1988) can cause CV to decline by over 50 % in *Gymnodinium sanguineum.* Changes in cell characteristics derived from chl *a* and in vivo fluorescence measurements can also be similar under various types of nutrient deficiency (e.g. Sakshaug & Holm-Hansen 1977). By comparing iron and nitrogen stress-mediated variation in such characteristics for *G. sanguineum* and other species in the literature, we can discern the specific effects of Fe stress with more confidence.

The current research shows that depletion of either iron or nitrogen in *Gymnodinium sanguineum* lowers Q_{chl} to between 20 and 25 % of nutrient-sufficient levels. Chl *a* is derived from the tetrapyrrole biosynthetic pathway (Garnick & Beale 1978), in which iron participates as a cofactor of certain enzymes and nitrogen is an important constituent of products occurring in the pathway (see Pushnik et al. 1984). Thus, it is not surprising that available data (e.g. Glover 1977, Guikema & Sherman 1983, Reuter & Ades 1987), including studies of Fe and N stress in a single species (this study, Sakshaug & Holm-Hansen 1977), demonstrate reduced Q_{chl} under either Fe or N deficiency for representatives of 5 algal groups.

The heme prosthetic group of photosynthetic electron transfer (PET) cytochromes is also a product of the tetrapyrrole biosynthetic pathway. In addition, PET processes require non-heme forms of Fe comprising iron-sulfur proteins such as ferredoxin (Jensen 1986). Given the involvement of Fe and N in the biosynthesis

Figs. 7 to 13. Iron-replete *Gymnodinium sanguineum.* NEPCC culture # D354. Fig. 7. Longitudinal section of protoplast showing the nucleus (N), an accumulation body (A), and cortical starch inclusions (S). Chloroplasts appear throughout the cell. Note vacuolate nature of cytoplasm. Scale bar = 10 µm. Fig. 8. Section exhibiting reticulate vacuole of pusule system (P) and peripheral regions of both flagellar openings (arrowheads). Note vesicle activity associated with flagellar canal (arrows). Scale bar = 2 µm. Fig. 9. Site of flagellar insertion with basal regions of both flagella (arrowheads) and one flagellar root (arrow) extending into adjacent cytoplasm. Note pusular vesicle (V) bordering on longitudinal flagellar canal (F). Scale bar = 1 µm. Fig. 10. Cross-section of flagellar canal (F) and associated pusular vesicles (V). Flagellar axoneme (arrowhead) and microtubule network (arrows) surrounding the canal are apparent. Scale bar = 0.5 µm. Fig. 11. Area containing extensive rough endoplasmic reticulum (ER), with several chloroplasts (C) and mitochondria (M) comprising characteristic close association of organelles. Note tubular cristae of mitochondria and similarity of matrix electron density to that of cytoplasm. Scale bar = 1 µm. Fig. 12. Portion of accumulation body with tightly packed contents showing 'fingerprint'-like pattern. Scale bar = 1 µm. Fig. 13. High magnification of chloroplast lamellae (L) consisting of 2 or 3 closely appressed thylakoids. Lamellae are highly organized with no evidence of thylakoid degeneration (cf. Figs. 15 and 16). Scale bar = 0.2 µm

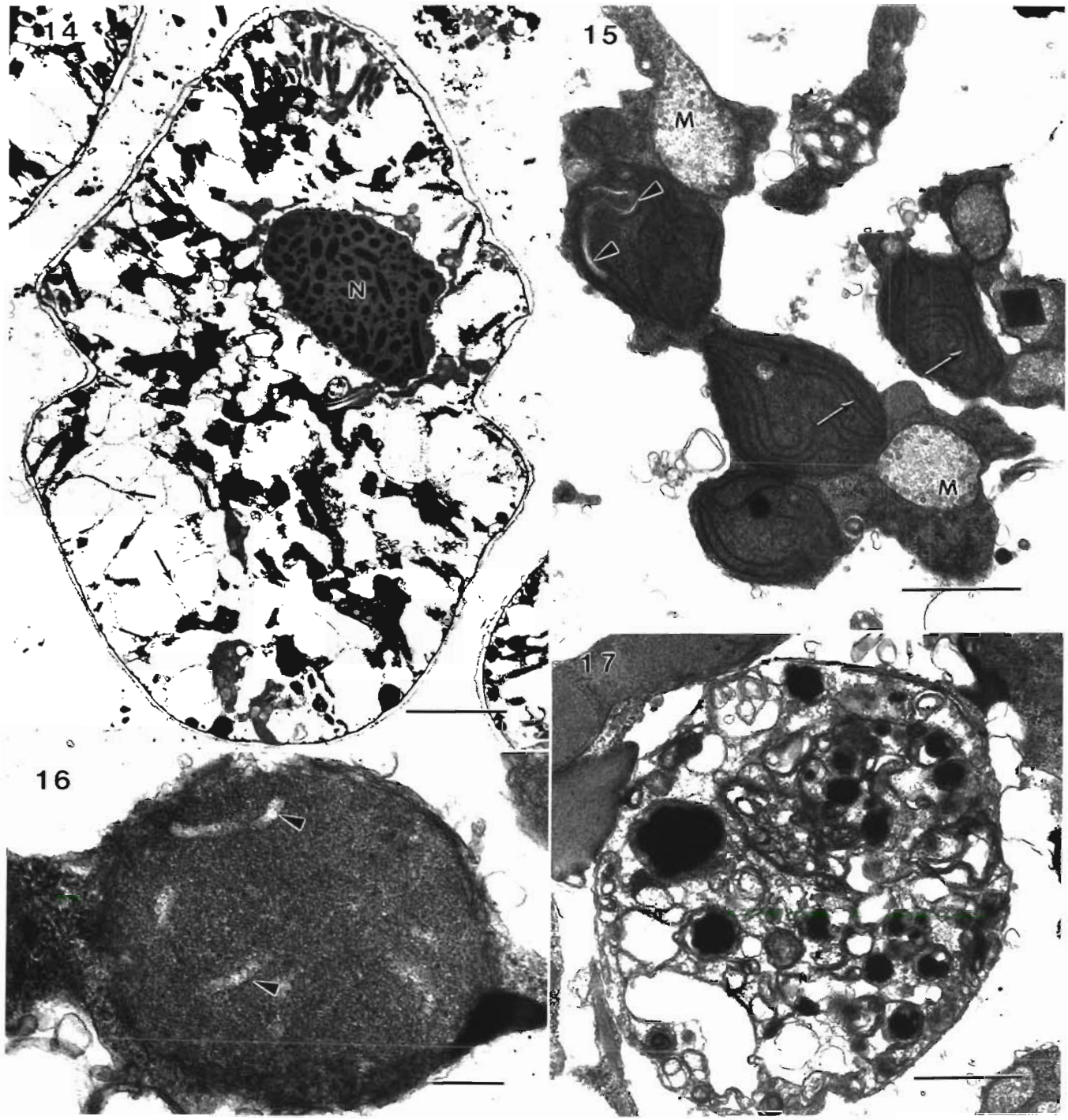

Figs. 14 to 17. Iron-deplete *Gymnodinium sanguineum*. NEPCC culture # D354. Fig. 14. Longitudinal section of protoplast containing nucleus (N) and highly vacuolate cytoplasm. Cytoplasmic area and general organelle abundance (e.g. chloroplasts) are reduced sharply from the iron-replete condition (cf. Fig. 7). Vacuolar regions appear divided by the tonoplast (arrows). Scale bar = 5 µm. Fig. 15. Association of organelles showing chloroplasts with 'normal' (arrows; note thylakoids occurring only in pairs) and structurally disrupted (arrowheads) lamellae (cf. Fig. 13). Mitochondria (M) exhibit a reduction in matrix electron density relative to cytoplasm (cf. Fig. 11). Scale bar = 1 µm. Fig. 16. Enlargement of chloroplast containing few, dilated thylakoids (arrowheads). Scale bar = 0.2 µm. Fig. 17. Accumulation body with loosely arranged contents exhibiting no apparent order (cf. Fig. 12). Scale bar = 1 µm

of PET components, and the functional relationship between PET reactions and in vivo fluorescence (Lawlor 1987), depletion of either nutrient might be expected to effect similar changes in F/chl *a*. Indeed, previous laboratory results generally demonstrate a 2- to 4-fold increase in this ratio above nutrient-sufficient values (e.g. Kiefer 1973, Sakshaug & Holm-Hansen 1977, Guikema & Sherman 1983), irrespective of limiting nutrient (i.e. Fe or N). However, if one considers the extreme cases of nutrient depletion in the present work, F/chl *a* of Fe-deplete *Gymnodinium sanguineum* increased 7 times compared to less than 3-fold for N-deplete cells. Even under conditions of severe nutrient limitation (Fig. 6), F/chl *a* was ca 2 times greater for Fe than N stress. Sakshaug & Holm-Hansen (1977) also observed larger Fe stress-mediated increases in this ratio compared to those associated with N depletion for the diatom *Skeletonema costatum*. Differences in F/chl *a*, coupled with similar chl *a* quotas for Fe- and N-stressed *G. sanguineum*, indicate a greater specific Fe stress-mediated response of in vivo fluorescence and thus PET activity.

Among the factors which may contribute to increases in F/chl *a* are enhanced light energy capture per unit pigment (i.e. specific absorption coefficient), and/or reduced efficiency of light energy transfer to photochemical reaction centers and of electron transport within the PET system. It is well documented that Fe-limited growth reduces both quantities of PET components (i.e. cytochromes and Fe-S proteins) and activity of the PET system in algae (Glover 1977, Sandmann & Malkin 1983, Sandmann 1985) and higher plants (Spiller & Terry 1980, Terry 1983). These specific effects on PET processes likely account, at least in part, for the difference in F/chl *a* between Fe- and N-deplete *Gymnodinium sanguineum*. Fluorescence may be augmented further by an increase in the specific chl *a* absorption coefficient through iron stress-mediated reductions in Q_{chl} (see discussion above) and thus in shelf-shading. However, it should be noted that increases in F/chl *a* associated with reduced nitrogen quotas have been suggested to result both from a rise in the specific absorption coefficient of chl *a* and also an uncoupling of photosynthesis (as reflected by lower quantum yields) in the diatom *Chaetoceros gracilis* (Cleveland & Perry 1987). While similar mechanisms may thus help to explain the F/chl *a* increase of N-deficient *G. sanguineum*, changes associated with iron stress are clearly more effective mediators of elevated in vivo fluorescence in this dinoflagellate.

Measurements of F_D/chl *a*, to the extent that F_D approximates the potential maximum in vivo fluorescence (F_{max}), provide further evidence that fluorescence properties of *Gymnodinium sanguineum* are more sensitive to iron than nitrogen deficiency. Application of the herbicide DCMU blocks PET between PSII and PSI, causing an increase in in vivo fluorescence to a larger (approximately maximum, Falkowski & Kiefer 1985) steady-state value (F_D) representing the energy otherwise available for PSII photochemistry (Prézelin 1981). If F_{max} under Fe and N stress were similar, little difference in F_D/chl *a* would be expected. Slovacek & Hannan (1977) have demonstrated previously that fluctuations in F/chl *a* induced by various forms of nutrient limitation can be eliminated by DCMU addition. However, exceptions to a constant fluorescence yield per unit chl *a* following DCMU application are not uncommon (e.g. Roy & Legendre 1979). In the case of *G. sanguineum*, variability between F_D/chl *a* ratios was less than exhibited by those of F/chl *a*. Nevertheless, F_D/chl *a* of Fe-deplete cells exceeded the N-deplete value by more than 1.5-fold, suggesting a greater F_{max} under iron stress.

In vivo fluorescence indices

In vivo fluorescence data (i.e. F and F_D/chl *a*) can be expressed as various indices which yield information largely about the operation of PSII. The following are three of these indices and the properties they are suggested to describe: (1) F/F_D, the proportion of captured light energy lost as fluorescence; (2) $1 - F/F_D$, the proportion of absorbed light energy utilized by PSII (i.e. the efficiency of PSII); and (3) $F_D - F$, the relative output of PSII (i.e. the capacity of PSII) (Prézelin 1981, Droop 1985). The preceding discussion has demonstrated that F/chl *a* and F_D/chl *a* (upon which these indices are based) are quite variable depending on species, growth conditions, and physiological state. The above 3 fluorescence indices therefore are sensitive to similar effects, but presumably are most useful in comparisons of different growth-limiting factors for one species under otherwise similar conditions (e.g. this study).

Data from the present work show increases in both F/chl *a* and F_D/chl *a* regardless of whether Fe or N limits growth. However, under conditions of Fe depletion, F increases to 60 % of F_D ($F/F_D = 0.61$), while remaining below 40 % of F_D for N depletion ($F/F_D = 0.38$). Conversely, the $1 - F/F_D$ indices are 0.39 and 0.62 for Fe and N depletion, respectively. The $F_D - F$ index (i.e. F_D/chl *a* − F/chl *a*) is equivalent for both Fe- and N-deplete cells ($F_D - F = 200$). Information provided by these in vivo fluorescence indices suggests that a greater proportion of harvested light energy is reemitted as fluorescence by iron-deplete *Gymnodinium sanguineum*. Further, while the capacity of PSII is affected similarly by either Fe or N depletion, the former reduces the photochemical efficiency of PSII to ca 60 %

of that maintained under the latter. Although such interpretations must be considered in light of the limitations associated with these indices, they are indeed consistent with a more pronounced effect of iron over nitrogen stress on PET processes for this species.

Ultrastructure

The general ultrastructural features of iron-replete *Gymnodinium sanguineum* are consistent with those described for other dinoflagellates (e.g. Dodge 1971). Of particular interest herein are changes in these characteristics associated with iron depletion and their relationship to the variation in chl *a* and in vivo fluorescence measurements discussed above. Perhaps the most obvious association is between the decline in Q_{chl} and decreased chloroplast number. This observation eliminates the possibility that lower chl *a* quotas are strictly a result of smaller chloroplasts. The size of those remaining chloroplasts may also have been reduced, but quantitative comparisons of Fe-replete and -deplete chloroplast dimensions were not made. Fewer chloroplasts present in Fe-deplete cells supports the argument for an increase in the chl *a* specific absorption coefficient due to reduced self-shading.

Degeneration of the normally well-organized chloroplast lamellae and thylakoids did occur under iron stress in *Gymnodinium sanguineum*, and similar effects have been reported for other algae (Meisch et al. 1980, Hardie et al. 1983, Doucette & Harrison 1989) and higher plants (Platt-Aloia et al. 1983). While functional interpretation of structural defects is generally lacking, the integrity of thylakoid membranes and their components clearly influences the efficiency of light harvesting as well as energy and electron transfer processes (Barber 1985). Thus, large in vivo fluorescence measurements of Fe-deplete cells may be at least partly explained by structural changes in photosynthetic membranes. The fact that many lamellae appear 'normal' (i.e. no structural disorders) suggests that alterations in photosynthetic components and processes are not necessarily manifested as obvious ultrastructural deviations.

Other changes noted in Fe-stressed protoplasts, such as increased vacuolar area, decreased mitochondrial matrix density and ER abundance, and variation in accumulation body morphology, may be non-specific responses to reduced growth rates. Unfortunately, no N-deplete cells were examined for comparison, as in the case of chl *a* and in vivo fluorescence. Thus, even the iron stress-mediated specificity of chloroplast degeneration is not certain, although a study of Fe- and N-starved *Agmenellum quadruplicatum* (Hardie et al. 1983) demonstrated that altered thylakoid structure was restricted to the former. Apart from chloroplasts, mitochondria might also be expected to exhibit specific Fe-mediated effects related to lower cytochrome production. Decreases in electron density of the matrix were encountered herein and for Fe-stressed *Alexandrium tamarense* (Doucette & Harrison 1989). Respiratory electron transport (RET) is associated with cristae membranes, which did not appear to change in either species. A more plausible explanation of lower matrix density in Fe-deplete mitochondria would be loss of TCA cycle constituents due to minimal energetic demands as growth rate declines.

Ecological considerations

Elucidation of nutritional factors affecting red tide population dynamics is essential to understanding the ecology of these natural phytoplankton blooms. To this end, indicators of nutrient limitation are of interest, since certain problems associated with their use may be minimized by the predominance of 1 or 2 species. Certain of these indicators exhibit considerable variation according to the nutrient and species in question. Indeed, a rigorous study of N and P limitation in 5 algal species (Healey & Hendzel 1979) revealed only 2 of 15 compositional and metabolic variables to be generally useful indicators of limitation by either nutrient.

In addition to the implication of increased iron bioavailability in promoting bloom formation (see 'Introduction'), a comparatively (cf. Brand et al. 1983) large iron requirement for 2 red tide dinoflagellates (Mueller 1985, Doucette & Harrison 1989, unpubl., this study) further suggests the potential importance of this trace metal in red tide ecology. Most characteristics of severely iron-limited cells monitored herein (pFe 21.2, 22.2) were easily distinguishable from those of nutrient-sufficient *Gymnodinium sanguineum*. Of several variables compared for both Fe- and N-limited growth, F/chl *a* was the most specific and sensitive indicator of iron limitation for this species. Perhaps employed in conjunction with other methods of assessing nutritional status (e.g. short-term nutrient enrichment; Healey 1979), the F/chl *a* ratio would be useful in detecting iron-stressed red tide populations. It must be recognized, however, that the present data reflect only nitrate-grown, Fe-limited cells of *G. sanguineum* and comparisons with those growing under N limitation. Thus, the generality of these findings in terms of both species and nutrient specificity requires further investigation.

Acknowledgements. We thank Drs M. Levasseur, N. Price, and P. Thompson for helpful discussions during preparation of this manuscript, N. Price for performing MINEQL calculations and W. Cochlan for data analysis using Curvefit. Reviewers' comments, especially those of W. Sunda, are greatly appreciated. We also acknowledge the expert technical assistance of

M. Weis. Support for this research was provided by a Natural Sciences and Engineering Research Council (NSERC) Postgraduate Scholarship and U.B.C. Graduate Fellowships awarded to G. J. D. and also by an NSERC strategic grant awarded to R. J. Andersen, P. J. H., and F. J. R. Taylor

LITERATURE CITED

Brand, L. E., Sunda, W. G., Guillard, R. R. L. (1983). Limitation of marine phytoplankton reproductive rates by zinc, manganese, and iron. Limnol. Oceanogr. 28: 1182–1198

Barber, J. (1985). Thylakoid membrane structure and organisation of electron transport components. In: Barber, J., Baker, N. R. (eds.) Photosynthetic mechanisms and the environment. Elsevier Sci. Publ., Amsterdam, p. 91–134

Cleveland, J. S., Perry, M. J. (1987). Quantum yield, relative specific absorption and fluorescence in nitrogen-limited *Chaetoceros gracilis*. Mar. Biol. 94: 489–497

Dandonneau, Y (1970). Un phénomène d'eaux rouges au large de Côte d'Ivoire causé par *Gymnodinium splendens* Lebour. Doc. Scient. Centre Rech. Océanogr. Abidjan 1 11–19

Dodge, J. D. (1971). Fine structure of the Pyrrophyta. Bot. Rev. 37: 481–508

Doucette, G. J. (1988). Aspects of iron and nitrogen nutrition in two red tide dinoflagellates, *Gymnodinium sanguineum* Hirasaka and *Protogonyaulax tamarensis* (Lebour) Taylor. Ph.D. thesis, University of British Columbia, Vancouver

Doucette, G. J., Harrison, P. J. (1989). Cyst formation in the red tide dinoflagellate *Alexandrium tamarense* (Dinophyceae): effects of iron stress. J. Phycol. 25: 721–731

Douglas, D., Peat, A., Whitton, B. A., Wood, P. (1986). Influence of iron status on structure of the cyanobacterium (blue-green alga) *Calothrix parietina*. Cytobios 47: 155–165

Droop, M. R. (1985). Fluorescence and the light/nutrient interaction in *Monochrysis*. J. mar biol. Ass. U.K. 65: 221–237

Falkowski, P., Kiefer, D. A. (1985). Chlorophyll *a* fluorescence in phytoplankton: relationship to photosynthesis and biomass. J. Plankton Res. 7: 715–731

Glover, H. (1977). Effects of iron deficiency on *Isochrysis galbana* (Chrysophyceae) and *Phaeodactylum tricornutum* (Bacillariophyceae). J. Phycol. 13: 208–212

Glover, H. (1978). Iron in Maine coastal waters; seasonal variation and its apparent correlation with a dinoflagellate bloom. Limnol. Oceanogr. 23: 534–537

Granick, S., Beale, S. I. (1978). Hemes, chlorophylls, and related compounds: biosynthesis and metabolic regulation. Adv. Enzymol. 46: 33–203

Guikema, J. A., Sherman, L. A. (1983). Organization and function of chlorophyll in membranes of cyanobacteria during iron starvation. Plant Physiol. 73: 250–256

Hardie, L. P., Balkwill, D. L., Stevens, S. E., Jr (1983). Effects of iron starvation on the ultrastructure of the cyanobacterium *Agmenellum quadruplicatum*. Appl. environ. Microbiol. 45: 1007–1017

Harrison, G. I., Morel, F. M. M. (1986). Response of the marine diatom *Thalassiosira weissflogii* to iron stress. Limnol. Oceanogr. 31: 989–997

Harrison, P. J., Waters, R. E., Taylor, F. J. R. (1980). A broad spectrum artificial seawater medium for coastal and open ocean phytoplankton. J. Phycol. 16: 28–35

Healey, F. P. (1979). Short-term responses of nutrient-deficient algae to nutrient addition. J. Phycol. 15: 289–299

Healey, F. P. (1980). Slope of the Monod equation as an indicator of advantage in nutrient competition. Microb. Ecol. 5: 281–286

Healey, F. P., Hendzel, L. L. (1979). Indicators of phosphorus and nitrogen deficiency in five algae in culture. J. Fish. Res. Bd Can. 36: 1364–1369

Hilt, K. L., Gordon, P. R., Hein, A., Caulfield, J. P., Falchuk, K. H. (1987). Effects of iron-, manganese-, or magnesium-deficiency on the growth and morphology of *Euglena gracilis*. J. Protozool. 34: 192–198

Holm-Hansen, O., Lorenzen, C. J., Holmes, R. W., Strickland, J. D. H. (1965). Fluorometric determination of chlorophyll. J. Cons. perm. int. Explor. Mer 30: 3–15

Ingle, R. M., Martin, D. F. (1971). Prediction of the Florida red tide by means of the iron index. Environ. Lett. 1. 69–74

Jensen, L. H. (1986). The iron-sulfur proteins: an overview. In: Matsubara, H., Katsube, Y., Wada, K. (eds.) Iron-sulfur protein research. Springer-Verlag, Berlin, p. 3–21

Kester, D. R. (1986). Equilibrium models in seawater: applications and limitations. In: Bernhard, M., Brinckman, F. E., Sadler, P. J. (eds.) The importance of chemical 'speciation' in environmental processes. Springer-Verlag, Berlin, p. 337–363

Kiefer, D. A. (1973). Chlorophyll *a* fluorescence in marine centric diatoms: responses of chloroplasts to light and nutrient stress. Mar Biol. 23: 39–46

Lawlor, D. W. (1987). Photosynthesis: metabolism, control, and physiology. J. Wiley & Sons, Inc., New York

Li, W. K. W (1983). Consideration of errors in estimating kinetic parameters based on Michaelis-Menten formalism in microbial ecology. Limnol. Oceanogr. 28: 185–190

Loftus, M. E., Seliger, H. H. (1975). Some limitations of the *in vivo* fluorescence technique. Chesapeake Sci. 16: 79–92

Meisch, H.-U., Becker, L. J. M., Schwab, D. (1980). Ultrastructural changes in *Chlorella fusca* during iron deficiency and vanadium treatment. Protoplasma 103: 273–280

Morel, F. M. M., Reuter, J. G., Anderson, D. M., Guillard, R. R. L. (1979). Aquil: a chemically defined phytoplankton culture medium for trace metal studies. J. Phycol. 15: 135–141

Mueller, B. (1985). Some aspects of iron limitation in a marine diatom. M.Sc. thesis, University of British Columbia, Vancouver

Murphy, L. S., Guillard, R. R. L., Brown, J. F. (1984). The effects of iron and manganese on copper sensitivity in diatoms: differences in the responses of closely related neritic and oceanic species. Biol. Oceanogr. 3: 187–201

Platt-Aloia, K. A., Thomson, W. W., Terry, N. (1983). Changes in plastid ultrastructure during iron nutrition-mediated chloroplast development. Protoplasma 114: 85–92

Prézelin, B. B. (1981). Light reactions in photosynthesis. In: Platt, T. (ed.) Physiological bases of phytoplankton ecology. Bull. Can. Dept. Fish. Oceans 210, p. 1–43

Pushnik, J. C., Miller, G. W., Manwaring, J. H. (1984). The role of iron in higher plant chlorophyll biosynthesis, maintenance and chloroplast biogenesis. J. Plant Nutr. 7: 733–758

Reuter, J. G., Ades, D. R. (1987). The role of iron nutrition in photosynthesis and nitrogen assimilation in *Scenedesmus quadricauda* (Chlorophyceae). J. Phycol. 23: 452–457

Reuter, J. G., Petersen, R. R. (1987). Micronutrient effects on cyanobacterial growth and physiology. N. Z. Jl mar. Freshwat. Res. 21: 435–445

Ringbom, A. (1963). Complexation in analytical chemistry. Chemical Analysis Monogr., Vol. 19. Interscience Publ., New York

Robinson, J. A., Characklis, W. G. (1984). Simultaneous estimation of V_{max}, K_m, and the rate of endogenous substrate

production (R) from substrate depletion data. Microb. Ecol. 10: 165–178

Robinson, M. G., Brown, L. N. (1983). A recurrent red tide in a British Columbia coastal lagoon. Can. J. Fish. Aquat. Sci. 40: 2135–2143

Rojas de Mendiola, B. (1979). Red tide along the Peruvian coast. In: Taylor, D. L., Seliger, H. H. (eds.) Toxic dinoflagellate blooms, Vol. I Elsevier North Holland, Inc., New York, p. 183–190

Roy, S., Legendre, L. (1979). DCMU-enhanced fluorescence as an index of photosynthetic activity in phytoplankton. Mar. Biol. 55: 93–101

Sakshaug, E., Holm-Hansen, O. (1977). Chemical composition of *Skeletonema costatum* (Grev.) Cleve and *Pavlova (Monochrysis) lutheri* (Droop) Green as a function of nitrate-, phosphate-, and iron-limited growth. J. exp. mar. Biol. Ecol. 29: 1–34

Sandmann, G. (1985). Consequences of iron deficiency on photosynthetic and respiratory electron transport in blue-green algae. Photosyn. Res. 6: 261–271

Sandmann, G., Malkin, R. (1983). Iron-sulfur centers and activities of the photosynthetic electron transport chain in iron-deficient cultures of the blue-green alga *Aphanocapsa*. Plant Physiol. 73: 724–728

Sillen, L. G., Martell, A. E. (1964). Stability constants of metal-ion complexes. Suppl. Chem. Soc. Lond., Spec. Publ. No. 17

Slovacek, R. E., Hannan, P. J (1977). In vivo fluorescence determinations of phytoplankton chlorophyll *a*. Limnol. Oceanogr. 22: 919–925

Spiller, S., Terry, N. (1980). Limiting factors in photosynthesis. II. Iron stress diminishes photochemical capacity by reducing the number of photosynthetic units. Plant Physiol. 65: 121–125

Steidinger, K. A., Haddad, K. (1981). Biologic and hydrographic aspects of red tides. Bioscience 31. 814–819

This article was presented by Dr D. K. Stoecker, Woods Hole, Massachusetts, USA

Tangen, K. (1979). Dinoflagellate blooms in Norwegian waters. In: Taylor, D. L., Seliger, H. H. (eds.) Toxic dinoflagellate blooms, Vol. 1. Elsevier North Holland, Inc., New York, p. 179–182

Taylor, F. J. R. (1987). Ecology of dinoflagellates. A. General and marine ecosystems. In: Taylor, F. J. R. (ed.) Biology of dinoflagellates. Blackwell Scientific Publications, Oxford, p. 398–502

Taylor, F. J. R. (1990). Phylum Dinoflagellata. In: Margulis, L., Corliss, J. O., Melkonian, M., Chapman, D. (eds.) Handbook of Protoctista. Jones & Bartlett Publishers, Inc., Boston, p. 419–437

Terry, N. (1983). Limiting factors in photosynthesis. IV. Iron stress-mediated changes in light-harvesting and electron transport capacity and its effects on photosynthesis *in vivo*. Plant Physiol. 71. 855–860

Verstreate, D. R., Storch, T. A., Dunham, V L. (1980). A comparison of the influence of iron on the growth and nitrate metabolism of *Anabaena* and *Scenedesmus*. Physiol. Plant. 50: 47–51

Westall, J. C., Zachary, J. L., Morel, F. M. M. (1976). MINEQL: a computer program for the calculation of chemical equilibrium composition of aqueous systems. Tech. Note No. 18, Ralph M. Parsons Laboratory for Water Resources and Environmental Engineering, Massachusetts Institute of Technology

Wood, E. D., Armstrong, F. A. J., Richards, F. A. (1967). Determination of nitrate in seawater by cadmium-copper reduction to nitrite. J. exp. mar. Biol. Ass. U.K. 47: 23–31

Yamochi, S. (1984). Nutrient factors involved in controlling the growth of red tide flagellates *Prorocentrum micans, Eutreptiella* sp. and *Chatonella marina* in Osaka Bay. Bull. Plankton Soc. Jpn 31: 97–106

Yentsch, C. M., Lewis, C. M., Yentsch, C. S. (1980). Biological resting in the dinoflagellate *Gonyaulax excavata*. Bioscience 30: 251–254

Manuscript first received: April 17, 1989
Revised version accepted: February 8, 1990